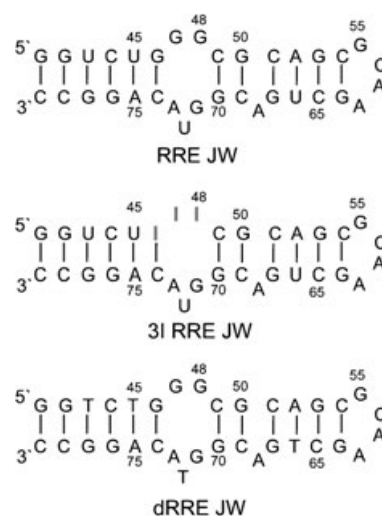


conjugates have been prepared in which the *cis*-Pt moiety has been tethered to high-affinity nucleic acid ligands (for example, acridine, ethidium bromide, peptides, and short oligonucleotides).<sup>[7]</sup> As part of our program aimed at advancing RNA as a drug target,<sup>[8]</sup> we have become interested in devising methods to “reverse” the nucleic acid selectivity of *cis*-Pt. Since RNA–protein complexes serve key functions in the life cycle of many retroviruses, RNA-selective delivery of reactive Pt<sup>II</sup> complexes may provide a novel mechanism for the inactivation of pathogen-specific RNA.

HIV-1 replication is critically dependent on the nuclear export of intron-containing viral RNA by the Rev protein.<sup>[9]</sup> The high-affinity Rev binding site within the Rev response element (RRE) is located at a G-rich bulge that is present in the minimized construct RRE JW shown in Figure 1.<sup>[10]</sup> Rev–



**Figure 1.** Secondary structures of the RRE constructs used. RRE JW is a minimized all-ribo Rev-binding RRE construct.<sup>[10]</sup> All-ribo 3I RRE JW contains three inosine (I) residues substituting the corresponding G residues. dRRE JW is an all-deoxyribo DNA analogue of RRE JW. The numbering used is in accordance with ref. [10].

## RNA-Selective Pt<sup>II</sup> Conjugates

### RNA-Selective Modification by a Platinum(II) Complex Conjugated to Amino- and Guanidinoglycosides\*\*

Jürgen Boer, Kenneth F. Blount, Nathan W. Luedtke, Lev Elson-Schwab, and Yitzhak Tor\*

Binding of the anticancer drug cisplatin (*cis*-Pt) to nucleic acids is believed to favor DNA over RNA.<sup>[1]</sup> Covalent modification of DNA produces intrastrand cross-links (at GpG, ApG, and GpNpG; N = A, C, G, or T),<sup>[2]</sup> and interstrand cross-links (at GG).<sup>[3]</sup> Cisplatin reacts with other cellular components including proteins,<sup>[4]</sup> phospholipids,<sup>[5]</sup> and small molecules.<sup>[6]</sup> To enhance DNA targeting, numerous

RRE recognition has served as an important paradigm for exploring the competitive inhibition of RNA–protein interactions.<sup>[11]</sup> Aminoglycoside antibiotics,<sup>[12]</sup> guanidinoglycosides,<sup>[13]</sup> and other small molecules that exhibit RNA over DNA selectivity have been shown to bind to the RRE and displace Rev through noncovalent interactions.<sup>[14]</sup> We hypothesized that, by using Pt<sup>II</sup> derivatives to covalently cross-link aminoglycosides and guanidinoglycosides to the RRE, viral RNA could be permanently damaged. Toward this end, we have developed RNA-selective Pt<sup>II</sup> conjugates. Herein we report the synthesis and RRE selectivity of two conjugates that, to our knowledge, represent the first examples of RNA-selective cross-linking agents.

Several criteria have guided the design of the glycoside–Pt<sup>II</sup> conjugates: a) Established RNA-selective scaffolds (for example, aminoglycosides or guanidinoglycosides) are chosen to secure preferential RNA over DNA binding; b) the polycationic scaffold is modified by substitution of a hydroxy group, rather than a chargeable group that is likely to be

[\*] Dr. J. Boer, Dr. K. F. Blount, N. W. Luedtke, L. Elson-Schwab, Prof. Dr. Y. Tor  
Department of Chemistry and Biochemistry  
University of California, San Diego  
La Jolla, CA 92093-0358 (USA)  
Fax: (+1) 858-534-0202  
E-mail: ytor@ucsd.edu

[\*\*] K.F.B. and J.B. contributed equally to this work. We thank the National Institutes of Health (Grant nos.: AI47673 to Y.T. and GM065652 to K.B.), the Universitywide AIDS Research Program (Grant no.: ID01-SD-027), and the Deutsche Forschungsgemeinschaft (postdoctoral fellowship to J.B.) for support.

Supporting information for this article is available on the WWW under <http://www.angewandte.org> or from the author.

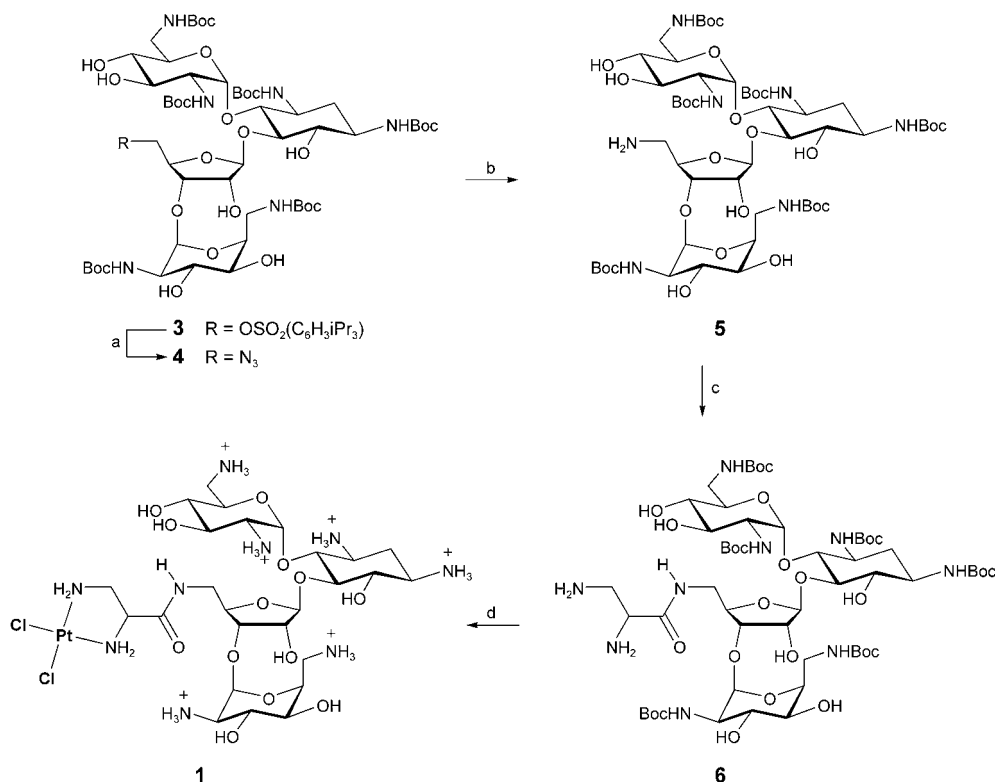
essential for RNA binding; c) a short linker between the Pt center and the RNA ligand is chosen to ensure enough conformational flexibility while maintaining proximity of the reactive metal center to the RNA-selective scaffold; and d) a chelating diamine is selected to secure Pt<sup>II</sup> coordination to the RNA-selective binder. With these considerations in mind, Pt<sup>II</sup> conjugates of neomycin B (**1**, Scheme 1) and guanidinoneomycin B (**2**, Scheme 2) were selected as our first-generation RNA-selective modifiers.

The synthesis of both derivatives starts with 5''-2,4,6-triisopropylbenzenesulfonate *N*-Boc-protected neomycin **3**.<sup>[15]</sup> Treatment of **3** with excess sodium azide affords the desired monoazide **4** in 89% yield (Scheme 1).<sup>[16]</sup> Catalytic hydrogenation of **4** quantitatively gives the corresponding amine **5**, which is coupled to *N*<sup>α</sup>,*N*<sup>β</sup>-di-Fmoc-(*S*)-2,3-diaminopropionic acid by using TBTU and HOBT. Cleavage of the Fmoc groups under basic conditions affords the neomycin derivative **6**, which presents a bidentate coordination site for platinum. Treatment with potassium tetrachloroplatinate in DMF/H<sub>2</sub>O leads to the formation of the fully protected aminoglycoside conjugate. Deprotection with 2 M HCl in dioxane/water affords the desired Pt<sup>II</sup> derivative **1** as the chloride salt in 95% yield (from **6**).<sup>[16]</sup>

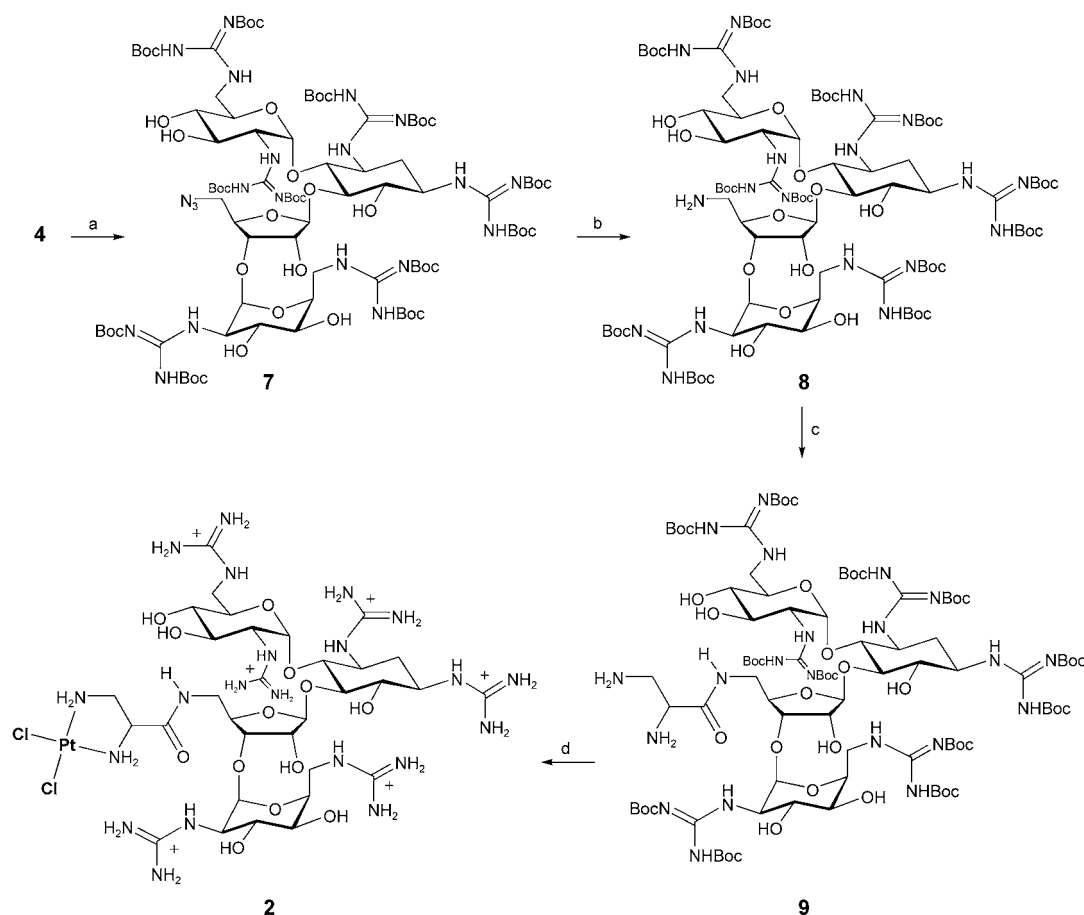
The 5''-azido neomycin derivative **4** is a common precursor for the synthesis of the neomycin–Pt<sup>II</sup> and guanidino-neomycin–Pt<sup>II</sup> conjugates, **1** and **2**, respectively. Thus, after removal of the six Boc protecting groups in **4** with 50% TFA/CH<sub>2</sub>Cl<sub>2</sub>, the crude 5''-azido neomycin is dissolved in MeOH/NEt<sub>3</sub> and treated with excess *N,N'*-di-Boc-*N''*-triflylguanidine, a powerful guanidinylation reagent.<sup>[17,18]</sup> Excess reagent is

readily removed, and the desired Boc-protected perguanidynylated 5''-azido neomycin **7** is obtained in excellent yield (99%; see Scheme 2). Reduction to the corresponding amine under Staudinger conditions provides **8** in 75% yield.<sup>[19]</sup> Condensation of the free amine with *N*<sup>α</sup>,*N*<sup>β</sup>-di-Fmoc-(*S*)-2,3-diaminopropionic acid by using TBTU/HOBT, followed by deprotection of the Fmoc groups with piperidine, gives **9** in 63% yield for the two steps. The reaction of the free chelating 1,2-diamino group with potassium tetrachloroplatinate in a two-phase CHCl<sub>3</sub>/H<sub>2</sub>O system, followed by TFA-mediated deprotection of the Boc groups, leads to the desired guanidynylated aminoglycoside–Pt<sup>II</sup> conjugate **2** as the TFA salt in 94% yield.<sup>[20]</sup>

To explore the ability of **1** and **2** to form covalent cross-links with RRE JW, denaturing polyacrylamide gel shift electrophoresis (DPAGE) has been utilized. Upon titration of RRE JW with **1** and **2**, DPAGE shows multiple retarded bands, a result indicating that the Pt<sup>II</sup> conjugates covalently bind the RRE (Figure 2a).<sup>[21]</sup> Addition of neomycin B, the parent aminoglycoside, produces no such effect (Figure 2b).<sup>[21]</sup> The reaction of **1** and **2** with the RRE is rapid and the adducts formed are stable under these denaturing conditions (Figure 2b).<sup>[22]</sup> According to DPAGE analysis, both conjugates covalently modify the RRE with comparable efficiencies (Figure 2a). Importantly, covalent modification takes place even in the presence of a vast excess of calf thymus DNA (CT DNA; Figure 2c). Approximately 5000-fold nucleotide excess of CT DNA must be added to prevent covalent-adduct formation between the platinated glycosides **1** and **2** and the RRE (Figure 2c). This competition experi-



**Scheme 1.** Synthesis of **1**: a) NaN<sub>3</sub>, DMF/H<sub>2</sub>O, 89%; b) H<sub>2</sub>, Pd/C, 99%; c) 1. *N*<sup>α</sup>,*N*<sup>β</sup>-di-Fmoc-(*S*)-2,3-diaminopropionic acid, TBTU, HOBT, 2,4,6-collidine, DMF; 2. piperidine, DMF, 80%; d) 1. K<sub>2</sub>PtCl<sub>4</sub>, DMF/H<sub>2</sub>O; 2. 2 M HCl/dioxane, 95%. Boc = *tert*-butoxycarbonyl, DMF = *N,N*-dimethylformamide, Fmoc = 9-fluorenylmethoxycarbonyl, HOBT = 1-hydroxy-1*H*-benzotriazole, TBTU = benzotriazol-1-yl-*N*-tetramethyluronium tetrafluoroborate.



**Scheme 2.** Synthesis of **2**: a) 1. TFA/CH<sub>2</sub>Cl<sub>2</sub>; 2. *N,N'*-di-Boc-*N''*-triflylguanidine, Et<sub>3</sub>N, MeOH, 99%; b) Ph<sub>3</sub>P, THF/H<sub>2</sub>O, 75%; c) 1. *N*<sup>α</sup>,*N*<sup>β</sup>-di-Fmoc-(*S*)-2,3-diaminopropionic acid, TBTU, HOBT, 2,4,6-collidine, DMF/CHCl<sub>3</sub>; 2. piperidine, DMF, 63%; d) 1. K<sub>2</sub>PtCl<sub>4</sub>, H<sub>2</sub>O/CH<sub>2</sub>Cl<sub>2</sub>, *n*Bu<sub>4</sub>NCl; 2. TFA/CH<sub>2</sub>Cl<sub>2</sub>, 94%. TFA = trifluoroacetic acid.

ment indicates a significant preference of these Pt<sup>II</sup>–glycoside conjugates for the RRE over CT DNA.

To explore the nature of the modification induced by the platinated conjugates, nonlabeled RRE JW (20 μM) was incubated with **1** (1.5 equiv) for 4 h, and the desalted reaction mixture was analyzed by MALDI-TOF mass spectrometry (Figure 3a,b). Under these conditions, the primary species observed (*m/z* 11914) represents a 1:1 covalent adduct, **1**·RRE, with both chloride ions displaced (expected *m/z* 11911).<sup>[23]</sup> Smaller amounts of both unmodified RRE JW (*m/z* 11023) and doubly conjugated (**1**)<sub>2</sub>·RRE (*m/z* 12806; expected *m/z* 12800) are also observed (Figure 3b). As shown in Figure 3c, a similar reactivity pattern is established for the guanidinoneomycin–Pt<sup>II</sup> conjugate **2** under the same conditions, where the dominant species observed is the singly conjugated product **2**·RRE (*m/z* 12164; expected *m/z* 12164). As with **1**, small amounts of the unmodified RRE JW and doubly modified product (**2**)<sub>2</sub>·RRE (*m/z* 13304; expected *m/z* 13303) are detected (Figure 3c). In contrast, treatment of **1** with 3I RRE JW or dRRE JW (see Figure 1 for sequences) under similar conditions does not yield a significant fraction of covalent adducts (not shown). Since neomycin displays lower affinity to these analogous nucleic acids than to RRE JW,<sup>[16]</sup> a correlation between specific binding and conjugation is implied.<sup>[24]</sup> When it is taken into account that

MALDI-TOF mass spectrometry is a strongly denaturing technique, these mass spectral data confirm the specific covalent-adduct formation of platinated glycosides to the all-ribo RRE JW.<sup>[25]</sup>

To identify the modification site of the Pt<sup>II</sup> conjugates **1** and **2** within RRE JW, the mixtures represented by the spectra in Figures 3b and c were 5'-<sup>32</sup>P-labeled and fractionated by using preparative 20% DPAGE. A representative purification gel is shown in Figure 3d. Whereas the **1**·RRE adduct ran as primarily one shifted band, addition of **2** to the RRE yielded two separable bands (marked **2**·RRE<sub>a</sub> and **2**·RRE<sub>b</sub>). Once labeled and isolated, these platinated RRE adducts were characterized by alkaline hydrolysis mapping (Figure 4). Covalent binding of the platinated glycosides to the RRE not only increases the mass of the RNA but also considerably diminishes its overall negative charge. This reduces the mobility of each hydrolyzed RNA fragment that contains the Pt<sup>II</sup> conjugate, whereas unmodified RNA fragments migrate identically to the hydrolyzed control. Thus, a discontinuity in the ladder points to the site of RNA–ligand conjugation. For **1**, this binding site is localized at the 3'-side of the tetraloop, a fact suggesting coordination to A<sub>62</sub>, A<sub>63</sub>, and G<sub>64</sub> (Figure 4a). This putative binding site is consistent with the coordination to purines that is seen for *cis*-Pt binding to DNA.<sup>[2a]</sup> Interestingly, a distinct gap is observed in the

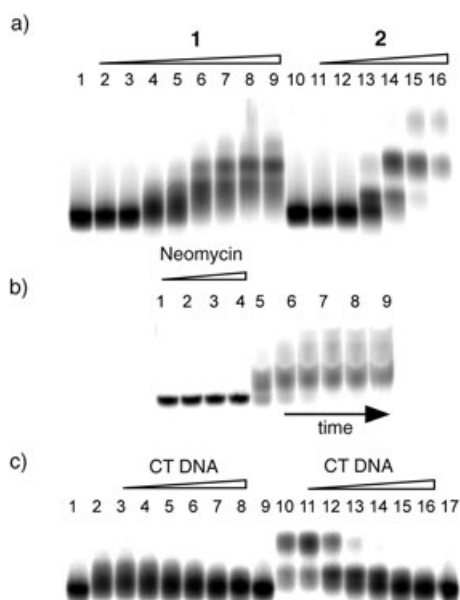


**Figure 2.** DPAGE radiogram with 25 nM 5'-<sup>32</sup>P-labeled RRE JW.<sup>[16]</sup> a) Lane 1: RNA only; lanes 2–9: increasing concentrations of **1** (0.050, 0.10, 0.50, 1.0, 2.5, 5.0, 7.5, and 10  $\mu$ M, respectively); lane 10: RNA only; lanes 11–16: increasing concentrations of **2** (0.050, 0.10, 0.50, 1.0, 2.5, and 5.0  $\mu$ M, respectively). b) Lanes 1–4: RNA with increasing concentrations of neomycin B (0.625, 1.25, 12.5, and 125  $\mu$ M, respectively); lanes 5–9: RNA with 625 nM of **1** after incubation (after 0.5, 1, 2, 3, 4 and 5 h, respectively). c) Lane 1: RNA only; lanes 2–8: RRE JW with 1  $\mu$ M **1** and increasing concentrations of calf thymus DNA (0, 8.5, 85, 425, 850  $\mu$ M, 4.25 and 8.5 mm base pairs, respectively); lane 9: RNA only; lanes 10–17: RRE JW with 1  $\mu$ M **2** and increasing calf thymus DNA (0, 8.5, 85, 425, 850  $\mu$ M, 4.25 and 8.5 mm base pairs, respectively).

hydrolytic map of **2**-RRE<sub>b</sub> (Figure 4a), a result that suggests an intramolecular cross-link between nucleosides at the boundaries of the gap, as has been previously observed for other RNA–RNA cross-links.<sup>[26]</sup> These results suggest the formation of an intramolecular cross-link between approximately G<sub>48</sub> and G<sub>67</sub>. This is consistent with the known propensity of *cis*-Pt to form cross-strand purine–purine cross-links.<sup>[2a]</sup> Examination of the NMR spectrum of the RRE reveals that the N7 positions of these two nucleotides are favorably placed for forming this interstrand cross-link (Figure 4c).<sup>[27]</sup>

In summary, new Pt<sup>II</sup> conjugates of neomycin B and guanidinoneomycin B are found to generate site-specific, RNA-selective, covalent cross-links to the RRE. The use of RNA-selective scaffolds, such as aminoglycosides or guanidinoglycosides, is demonstrated to impart the necessary RNA selectivity upon the *cis*-Pt moiety. This observation serves as an important precedent for the selective covalent modification of therapeutically relevant RNA targets.

### Experimental Section

**RNA:** Oligonucleotides were purchased from Dharmacon Research, deprotected, and purified by using standard protocols. A solution of calf thymus DNA was purchased from Gibco BRL (catalogue no.: 15633-019) and quantified by using an average extinction

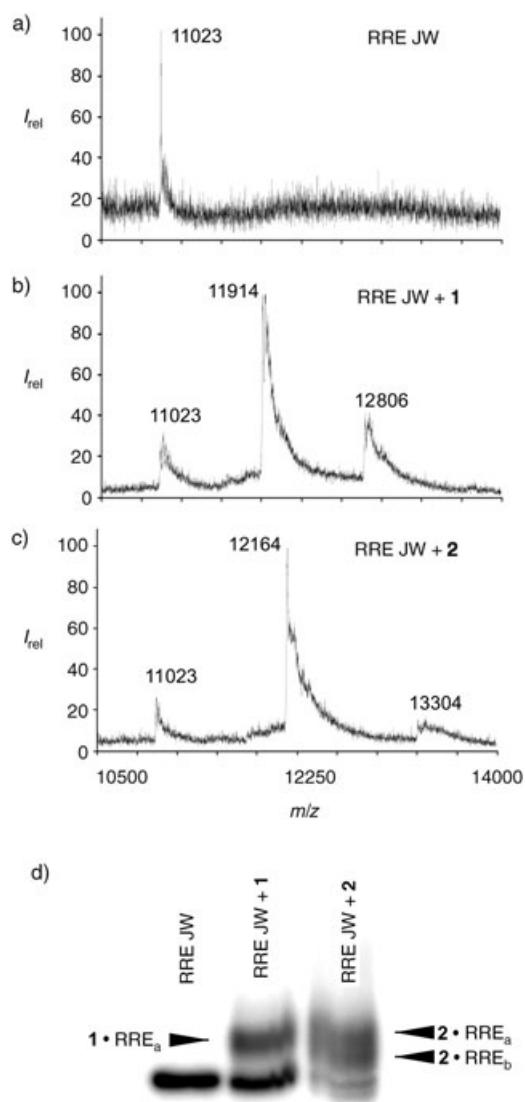


**Figure 3.** MALDI-TOF MS analysis of 20  $\mu$ M RRE JW a) alone, b) with 30  $\mu$ M of **1**, and c) with 20  $\mu$ M of **2**. See the Experimental Section for procedures. d) Denaturing gel purification of 5'-<sup>32</sup>P-labeled RRE JW and RRE JW adducts. The two adducts isolated are indicated (**2**-RRE<sub>a</sub> and **2**-RRE<sub>b</sub>).

coefficient of 6550 cm<sup>-1</sup>M<sup>-1</sup> per base. The extinction coefficient for all RRE JW constructs was calculated as 371 000 cm<sup>-1</sup>M<sup>-1</sup>.

**DPAGE analysis:** For evaluating the cross-linking ability of **1** and **2**, RNA was prefolded by being heated to 65 °C for 5 minutes and then cooled to room temperature for 20 min. A final concentration of 25 nM prefolded RRE JW containing a trace of 5'-<sup>32</sup>P-labeled RRE JW ( $\approx$  5000 cpm) was then incubated with the indicated amount of **1** or **2** in 10 mM sodium phosphate buffer (pH 7.0) containing 100 mM sodium perchlorate. Where appropriate, calf thymus DNA was added to the folded RRE JW prior to the addition of **1** or **2**. After 2 h at room temperature, cross-linking reactions were diluted with an equal volume of formamide loading dye, heated to 90 °C for 3 min, and loaded immediately onto a 20% denaturing polyacrylamide gel.

**MALDI-TOF MS experiments:** A solution of RRE JW (75  $\mu$ L of a 40  $\mu$ M solution) in 10 mM tris(hydroxymethyl)aminomethane (Tris; pH 7.5) with 50 mM NaCl was heated to 65 °C for 5 min and cooled at room temperature for 20 min. This solution was diluted with

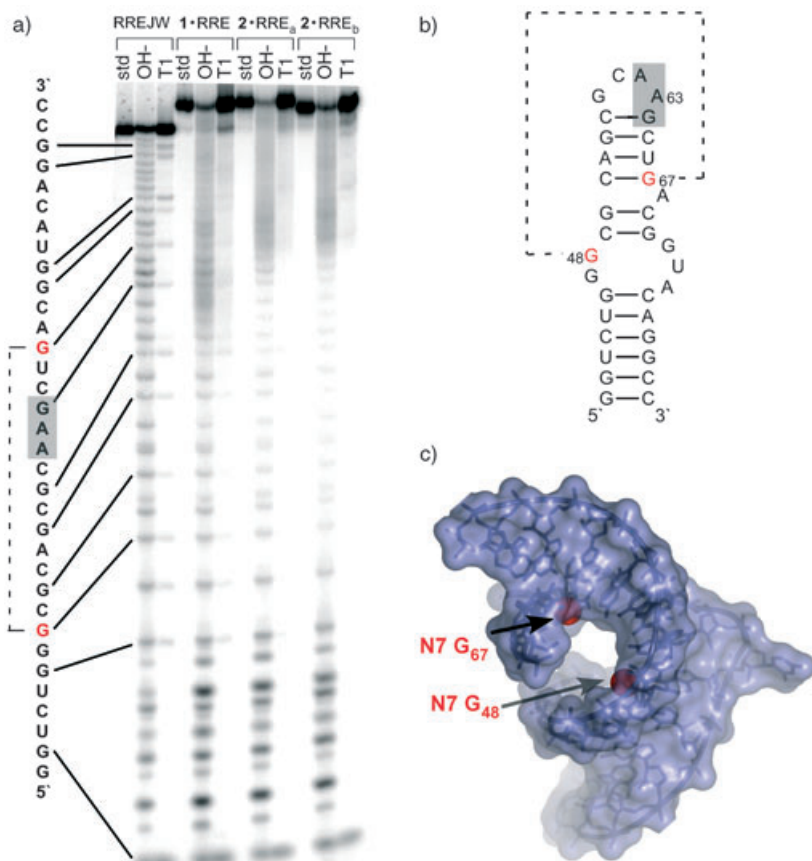


**Figure 4.** Alkaline hydrolytic footprint of RRE JW and its platinated adducts.<sup>[16]</sup> a) “std” lanes are untreated RNA, “OH” lanes show RNA after alkaline hydrolysis, and “T1” lanes show RNA after cleavage by ribonuclease T1 under denaturing conditions. The conjugation site of **1** is shaded. An interstrand cross-link (dotted line) is observed between approximately G<sub>48</sub> and G<sub>67</sub> (shown in red). b) Conjugation sites are shown in the context of the secondary structure of RRE JW. c) The three-dimensional structure of the RRE reveals that the N7 positions of G<sub>48</sub> and G<sub>67</sub> (red space-filling representation) are near each other in space and well-positioned for forming an interstrand cross-link.

phosphate/perchlorate buffer (75  $\mu\text{L}$ ) to yield final concentrations of 10 mM sodium phosphate (pH 7.4), 100 mM sodium perchlorate, and either 30  $\mu\text{M}$  **1** or 20  $\mu\text{M}$  **2**. These reaction mixtures were incubated at room temperature for 4 h, at which point they were desalted by passing through a G-25 spin column (Amersham-Pharmacia) that had been equilibrated with water. After desalting, the reactions were lyophilized overnight and resuspended in water (20  $\mu\text{L}$ ). To confirm the addition of platinated conjugates, an aliquot was fractionated on a 20% PAGE gel and visualized with Stains-all (Acros). For MALDI-TOF MS analysis, 2  $\mu\text{L}$  of each sample was combined with 1  $\mu\text{M}$  ammonium citrate buffer (PE Biosystems), 1  $\mu\text{L}$  of 75  $\mu\text{M}$  DNA standard (5'-AGGCATGCAAGCTTGAGTATTCTAT-3'), and 6  $\mu\text{L}$  of saturated 3-hydroxypicolinic acid. After desalting with an ion-exchange resin (PE Biosystems), the sample was spotted onto a gold-coated MALDI plate and dried on a 55°C heat block. MALDI-TOF spectra were collected on a PE Biosystems Voyager-DE STR MALDI-TOF spectrometer in positive-ion, delayed-extraction mode. By calibrating all spectra relative to the +1 and +2 ions of the internal DNA standard, the observed mass of RRE JW and its adducts should have a resolution of  $\pm 4$  mass units.

Footprinting analysis: **1-RRE** and **2-RRE** (3  $\mu$ L) from the MALDI-TOF MS analysis described above were labeled with T4 polynucleotide kinase (New England Biolabs) and purified by using standard protocols.<sup>[16]</sup> Purified RNA adducts were resuspended

in water (50  $\mu\text{L}$ ). Alkaline hydrolysis reactions were conducted in a 50 mM sodium bicarbonate buffer (pH 9.0; total volume 8  $\mu\text{L}$ ) and contained 5'- $^{32}\text{P}$ -labeled RRE JW ( $\approx 60000$  cpm). These reactions were heated to 90°C for 6.5 min and immediately quenched on ice for 10 min. Following a brief spin, samples were 1:1 diluted with formamide loading dye and 1.5  $\mu\text{L}$  were loaded onto a 20% polyacrylamide gel. Ribonuclease T1 reactions contained 38000 cpm of each RRE JW adduct and 1 unit of ribonuclease T1 (Boehringer Mannheim) in a solution of 20 mM sodium citrate (pH 5.0), 1 mM ethylenediaminetetraacetate (EDTA), 3 M urea, and 0.04  $\mu\text{g}\mu\text{L}^{-1}$  yeast torula RNA (Ambion). These reactions were incubated at 65°C for 30 minutes, then diluted into an equal volume of formamide loading dye and separated with 20% denaturing polyacrylamide gels. All gels were run for approximately 3 h at 15 W and analyzed by using a Molecular Dynamics Storm Phosphorimager.

**Keywords:** aminoglycosides · antiviral agents · drug design · platinum · RNA

- [1] E. R. Jamieson, S. J. Lippard, *Chem. Rev.* **1999**, 99, 2467–2498.
- [2] a) A. M. J. Fichtinger-Schepman, J. L. van der Veer, J. H. J. den Hartog, P. H. M. Lohman, J. Reedijk, *Biochemistry* **1985**, 24, 707–713; b) A. Eastman, *Biochemistry* **1986**, 25, 3912–3915.
- [3] H. Huang, J. Woo, S. C. Alley, P. B. Hopkins, *Bioorg. Med. Chem.* **1995**, 3, 659–669.
- [4] R. N. Bose, *Mini-Rev. Med. Chem.* **2002**, 2, 103–111.
- [5] G. Speelmans, R. W. Staffhorst, K. Versluis, J. Reedijk, B. de Kruijff, *Biochemistry* **1997**, 36, 10545–10550.
- [6] T. Ishikawa, F. Ali-Osman, *J. Biol. Chem.* **1993**, 268, 20116–20125.
- [7] Selected examples: a) B. E. Bowler, L. S. Hollis, S. J. Lippard, *J. Am. Chem. Soc.* **1984**, 106, 6102–6104; b) B. D. Palmer, H. H. Lee, P. Johnson, B. C. Baguley, G. Wickham, L. P. G. Wakelin, W. D. McFadyen, W. A. Denny, *J. Med. Chem.* **1990**, 33, 3008–3014; c) D. Gibson, K. F. Gean, J. Katzhendle, R. Ben-Shoshan, A. Ramu, I. Ringel, *J. Med. Chem.* **1991**, 34, 414–420; d) J. Whittaker, W. D. McFadyen, G. Wickham, L. P. Wakelin, V. Murray, *Nucleic Acids Res.* **1998**, 26, 3933–3939; e) L. C. Perrin, C. Culliname, W. D. McFayden, D. R. Phillips, *Anti-Cancer Drug Des.* **1999**, 14, 243–252; f) Y. S. Chen, M. J. Heeg, P. G. Brauschweiger, W. H. Xie, P. G. Wang, *Angew. Chem.* **1999**, 111, 1882–1884; *Angew. Chem. Int. Ed.* **1999**, 38, 1768–1769; g) M. S. Robillard, A. R. P. M. Valentijn, N. J. Meeuwenoord, G. A. van der Marel, J. H. van Boom, J. Reedijk, *Angew. Chem.* **2000**, 112, 3226–3229; *Angew. Chem. Int. Ed.* **2000**, 39, 3096–3099; h) Y. Mikata, Y. Shinohara, K. Yoneda, Y. Nakamura, I. Brudzinska, T. Tanase, T. Kitayama, R. Takagi, T. Okamoto, I. Kinoshita, M. Doe, C. Orvig, S. Yano, *Bioorg. Med. Chem. Lett.* **2001**, 11, 3045–3047; i) S. K. Sharma, L. W. McLaughlin, *J. Am. Chem. Soc.* **2002**, 124, 9658–9659; j) M. S. Robillard, N. P. Davies, G. A. van der Marel, J. H. van Boom, J. Reedijk, V. Murray, *J. Inorg. Biochem.* **2003**, 96, 331–338; k) R. J. Heetebrij, M. de Kort, N. J. Meeuwenoord, H. den Dulk, G. A. van der

- Marel, J. H. van Boom, J. Reedijk, *Chem. Eur. J.* **2003**, *9*, 1823–1827.
- [8] a) Y. Tor, *ChemBioChem* **2003**, *4*, 998–1007; b) N. W. Luedtke, Y. Tor in *Small Molecule DNA and RNA Binders: From Synthesis to Nucleic Acid Complexes* (Eds.: M. Demeunynck, C. Bailly, D. Wilson), Wiley-VCH, Weinheim, **2003**, pp. 18–40.
- [9] a) V. W. Pollard, M. H. Malim, *Annu. Rev. Microbiol.* **1998**, *52*, 491–532; b) A. D. Frankel, J. A. T. Young, *Annu. Rev. Biochem.* **1998**, *67*, 1–25.
- [10] J. L. Battiste, H. Mao, N. S. Rao, R. Tan, D. R. Muhandiram, L. E. Kay, A. D. Frankel, J. R. Williamson, *Science*, **1996**, *273*, 1547–1551.
- [11] N. W. Luedtke, Y. Tor, *Biopolymers* **2003**, *70*, 103–119.
- [12] M. L. Zapp, S. Stern, M. R. Green, *Cell* **1993**, *74*, 969–978.
- [13] N. W. Luedtke, T. J. Baker, M. Goodman, Y. Tor, *J. Am. Chem. Soc.* **2000**, *122*, 12035–12036.
- [14] K. Li, T. M. Davis, C. Bailly, A. Kumar, D. W. Boykin, W. D. Wilson, *Biochemistry* **2001**, *40*, 1150–1158.
- [15] a) K. Michael, H. Wang, Y. Tor, *Bioorg. Med. Chem.* **1999**, *7*, 1361–1371; b) S. R. Kirk, N. W. Luedtke, Y. Tor, *J. Am. Chem. Soc.* **2000**, *122*, 980–981.
- [16] See the Supporting Information for detailed experimental procedures and additional data.
- [17] T. J. Baker, N. W. Luedtke, Y. Tor, M. Goodman, *J. Org. Chem.* **2000**, *65*, 9054–9058.
- [18] We have found it is beneficial to install the guanidinium groups at early stages of the synthetic scheme.
- [19] Attempts to reduce the azide by catalytic hydrogenation, a method that was successfully employed for **4**, led to several by-products.
- [20] Both cisplatin conjugates were fully characterized by ESI mass spectrometry and 1D and 2D  $^1\text{H}$  and  $^{13}\text{C}$  NMR spectroscopy, as well as by  $^{195}\text{Pt}$  NMR spectroscopy.<sup>[16]</sup> Importantly, the  $^{195}\text{Pt}$  NMR spectra show a single peak at  $\delta = -2360$  and  $-2361$  ppm, for **1** and **2**, respectively; this indicates a  $[\text{Cl}_2\text{PtN}_2]$  coordination sphere.
- [21] Noncovalent complexes are denatured under such conditions and yield no gel-mobility shift. See, for example, Figure 2b which illustrates the case with neomycin B (a molecule that is known to associate with the RRE noncovalently).
- [22] Note that displacement experiments with BODIPY-labeled neomycin and  $\text{CN}^-$ -treated **1** and **2** indicate that these derivatives have approximately the same affinity to the RRE JW compared to the nonmodified parent compounds (neomycin B and guanidinoneomycin B, respectively).<sup>[16]</sup> This indicates that the conjugated metal center does not significantly alter the RNA-binding characteristics of the glycoside skeleton.
- [23] The unmodified RNA ( $m/z$  11023) plus **1** (964 for  $\text{C}_{26}\text{H}_{53}\text{N}_9\text{O}_{13}\text{PtCl}_2$ ) minus two chloride ions (70) yields an expected mass of  $m/z$  11917. Since the aminoglycoside carries six positive charges under the acidic conditions of the matrix used, six fewer protons are required to form a single-charged positive ion of the Pt-conjugated RRE JW. For an oligonucleotide of this size, MALDI-TOF MS can be expected to show an accuracy of  $\pm 4$  amu. As such, good agreement between the expected and experimentally observed mass is established.
- [24] Similar mass spectral characterization of **2** with the RRE reveals its binding and covalent modification are slightly less specific than those of **1**. This agrees with a previous determination of the RRE-binding specificity of amino- and guanidinoglycosides<sup>[13]</sup> and underscores the link between specific binding and platinum conjugation to the RNA.
- [25] Since the mass spectra indicate that both chloride ions are displaced, a similar mechanism to the coordination of *cis*-Pt to DNA is implied.
- [26] L. Wang, D. E. Ruffner, *Nucleic Acids Res.* **1997**, *25*, 4344–4361.
- [27] J. A. Ippolito, T. A. Steitz, *J. Mol. Biol.* **2000**, *295*, 711–717.